Comparative research on the transmission-mode GaAs photocathodes of exponential-doping structures*

Chen Liang(陈 亮)[a)b)†], Qian Yun-Sheng(钱芸生)[b)],
Zhang Yi-Jun(张益军)[b)], and Chang Ben-Kang(常本康)[b)]

[a)] *Institute of Optoelectronics Technology, China Jiliang University, Hangzhou* 310018, *China*

[b)] *Institute of Electronic Engineering & Optoelectronics Technology, Nanjing University of Science and Technology, Nanjing* 210094, *China*

(Received 13 January 2011; revised manuscript received 23 August 2011)

Early research has shown that the varied doping structures of the active layer of GaAs photocathodes have been proven to have a higher quantum efficiency than uniform doping structures. On the basis of our early research on the surface photovoltage of GaAs photocathodes, and comparative research before and after activation of reflection-mode GaAs photocathodes, we further the comparative research on transmission-mode GaAs photocathodes. An exponential doping structure is the typical varied doping structure that can form a uniform electric field in the active layer. By solving the one-dimensional diffusion equation for no equilibrium minority carriers of transmission-mode GaAs photocathodes of the exponential doping structure, we can obtain the equations for the surface photovoltage (SPV) curve before activation and the spectral response curve (SRC) after activation. Through experiments and fitting calculations for the designed material, the body-material parameters can be well fitted by the SPV before activation, and proven by the fitting calculation for SRC after activation. Through the comparative research before and after activation, the average surface escape probability (SEP) can also be well fitted. This comparative research method can measure the body parameters and the value of SEP for the transmission-mode GaAs photocathode more exactly than the early method, which only measures the body parameters by SRC after activation. It can also help us to deeply study and exactly measure the parameters of the varied doping structures for transmission-mode GaAs photocathodes, and optimize the Cs–O activation technique in the future.

Keywords: GaAs photocathode, surface photovoltage, electron diffusion length, surface escape probability

PACS: 42.70.Gi, 71.55.Eq, 72.10.–d **DOI:** 10.1088/1674-1056/21/3/034214

1. Introduction

Negative electron affinity (NEA) GaAs photocathodes have already been found to have wide applications in night-vision image intensifiers and to be potential sources for next-generation electron accelerators due to their high spin polarization, low energy spread, good emitting efficiency, low dark emission and narrow energy spread. In most practical application areas, the photocathodes must be operated in the transmission mode. In practice, the properties of GaAs photocathodes depend mainly on three factors, the electron diffusion length, the back-interface recombination velocity and the value of surface escape probability (SEP) after activation. The first two factors are related to the internal properties of photocathode materials, and the last one is related mainly to the crystal face, the surface cleaning technique and the Cs–O activation procedure.[1−4]

In accordance with the three-step photoemission model, which states that the photo-excited electrons can be emitted to vacuum through optical absorption, electron transport to the surface and tunneling through the surface barriers, we designed exponential doping structures to investigate the internal properties for transmission-mode GaAs photocathode material.[4] The exponential doping structure exhibits an exponential variation in doping concentration downwards from the internal body to the surface, in which the surface doping concentration is lower than the bulk concentration and therefore a downward band bending region from the GaAs bulk to the surface is formed by the Fermi-level leveling effect. This band bending region can correspond to a positive electric field, within which the photoelectrons may move toward surface barriers in two ways: concentration diffusion and internal electric field drift, so the transport

*Project supported by the National Natural Science Foundation of China (Grant Nos. 60678043 and 60801036).
†Corresponding author. E-mail: sunembed@yahoo.com.cn
© 2012 Chinese Physical Society and IOP Publishing Ltd

distance of photo-excited electrons from bulk to surface will thereby be enhanced, which can finally improve the emitted quantum efficiency of NEA GaAs photocathodes.[5]

In early studies, many of the main parameters such as electron diffusion length, active layer thickness, back-interface recombination and surface escape probability have been studied thoroughly through the spectral response curve (SRC) after activation for GaAs photocathodes. The surface photovoltage (SPV) curve before activation is related only to the properties of the body materials, and cannot be inflected by the Cs–O activations and the surface barriers. In this paper, we deduce the surface photovoltage equations and spectral response equations for the transmission-mode GaAs photocathodes of the exponential doping structure, considering the back-interface recombination velocity, active layer thickness and built-in electric field. Through experiments on the designed transmission-mode material, the body parameters of the transmission-mode photocathode can be well fitted by the SPV before activation. Through the fitting calculation for SRC after activation, the values of the body parameters can be well proved, and the surface escape probability value can also be well fitted by comparative research before and after activation. The comparative research is shown to be a better method to accurately study the varied doping structures for transmission-mode GaAs photocathodes, which can help us to optimize the varied doping designs in the future.[5]

2. The principle of transmission-mode photocathodes

An exponential doping structure is where the p-type doping concentrations of the active layers vary from body to surface following the exponential equation[6]

$$N(x) = N_0 \exp(-Ax), \tag{1}$$

where x is the distance between a point in the active layer and the back interface, A is the exponential doping coefficient, N_0 is the initial doping concentration of the back interface, and $N(x)$ is the doping concentration at the distance of x.

As a result of the exponential doping structure, a constant built-in electric field with direction from back interface to surface is formed, which can be expressed as[7,8]

$$\begin{aligned} V(x) &= \frac{kT}{q} \ln \frac{N_0}{N(x)} \\ &= \frac{k_0 T}{q} \ln \frac{N_0}{N_0 \exp(-Ax)} == \frac{k_0 TAx}{q}, \\ E(x) &= -\frac{\mathrm{d}V(x)}{\mathrm{d}x} = -\frac{k_0 TA}{q}, \end{aligned} \tag{2}$$

where k is the Boltzmann constant, T is the absolute temperature, q is the electronic charge, $V(x)$ is the internal electric voltage, and $E(x)$ is the electric field intensity. From Eq. (2), the relationship between x and $V(x)$ is shown in Fig. 1, where d is the depth of the exponential doping layer.

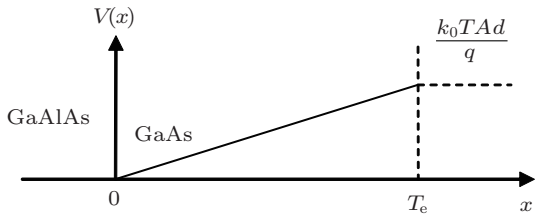


Fig. 1. The built-in electric field of exponential doping GaAs photocathodes.

As the electric potential is directly proportional to $V(x)$, a continuously downward band structure from the GaAs bulk to the surface is formed in the photocathodes, as shown in Fig. 2. The band offset near the back interface is due to the block barrier formed because the band gap of GaAlAs is larger than that of GaAs, and the surface band bending and surface barriers are the result of the Cs–O activation for p-mode GaAs material.[9]

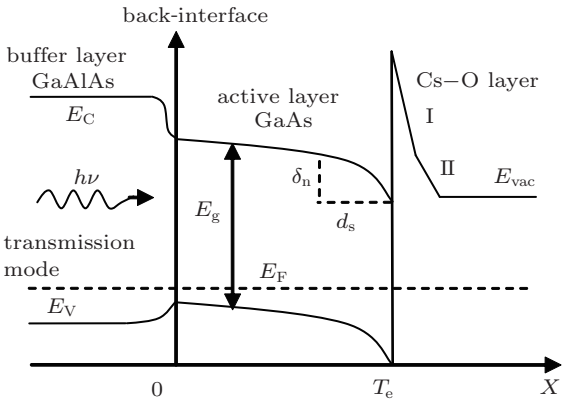


Fig. 2. The band structure of exponential doping GaAs photocathodes. E_{C} is the conduction-band minimum, E_{V} is the valence band maximum, E_{g} is the band gap, E_{F} is the Fermi level, E_{vac} is the vacuum level, and δ_{n} and d_{s} are the height and width of the surface band bending region.

In consideration of the built-in electric field and the active layer thickness, the one-dimensional diffusion equation for no equilibrium minority carriers of transmission-mode GaAs photocathodes is given as[10,11]

$$D_{\mathrm{n}} \frac{\mathrm{d}^2 n(x)}{\mathrm{d}x^2} - \frac{n(x)}{\tau} + \alpha_{h\nu} I_0 (1-R) \exp(-\alpha_{h\nu} x) = 0,$$

$$x \in [0, T_{\rm e}]\,. \tag{3}$$

For exponential doping GaAs photocathodes, the boundary condition is shown as

$$\begin{aligned} &D_{\rm n}\frac{{\rm d}n(x)}{{\rm d}x} - \mu\,|E|\,n(x)\,|_{x=0} = S_{\rm V} n(x)\,|_{x=0}\,,\\ &n(T_{\rm e}) = 0, \end{aligned} \tag{4}$$

where $D_{\rm n}$ is the electron diffusion coefficient, τ is the electron lifetime, $T_{\rm e}$ is the active layer thickness, $\alpha_{h\nu}$ is the absorption coefficient, $S_{\rm V}$ is the back-interface recombination velocity, and μ is the electron mobility.

According to diode theory, the surface photovoltage is shown as

$$\begin{aligned} &\Delta V = \frac{kT}{q}\ln\left(1+\frac{j_{\rm w}}{c}\right), \quad J_{\rm w} = D_{\rm n}\frac{{\rm d}n(x)}{{\rm d}x}\,|_{x=T_{\rm e}}\,,\\ &J = PD_{\rm n}\frac{{\rm d}n(x)}{{\rm d}x}\,|_{x=T_{\rm e}}\,, \end{aligned} \tag{5}$$

where ΔV is the surface photovoltage for the GaAs photocathode, $J_{\rm w}$ is the photo-electron current flowing to the surface barrier from the internal body, J is the spectrum response current flowing to the vacuum after Cs-O activation, and P is the SEP. The relationship between different coefficients is shown as

$$D_{\rm n}/\mu_{\rm n} = kT/q, \quad L_{\rm D} = \sqrt{D_{\rm n}\tau}. \tag{6}$$

Thus, the surface photovoltage $\Delta V_{\rm vd}$ and the spectral response $J_{\rm vd}$ equations for the exponential doping materials could be deduced from Eqs. (3)–(5), and they are expressed as[12]

$$\begin{aligned} \Delta V_{\rm vd} =\ & \frac{kTI_0(1-R)\alpha_{h\nu}L_{\rm D}}{qc(\alpha_{h\nu}^2 L_{\rm D}^2 + \alpha_{h\nu}{\rm L_E} - 1)}\\ &\times\left\{\frac{N(S+\alpha_{h\nu}D_{\rm n})}{M}\times\exp(L_{\rm E}T_{\rm e}/2L_{\rm D}^2)\right.\\ &\left.-\frac{Q\exp(-\alpha_{h\nu}T_{\rm e})}{M} - \alpha_{h\nu}L_{\rm D}\exp(-\alpha_{h\nu}T_{\rm e})\right\}, \end{aligned} \tag{7}$$

$$\begin{aligned} J_{\rm vd} =\ & \frac{PI_0(1-R)\alpha_{h\nu}L_{\rm D}}{\alpha_{h\nu}^2 L_{\rm D}^2 - \alpha_{h\nu}{\rm L_E} - 1}\\ &\times\left\{\frac{N(S+\alpha_{h\nu}D_{\rm n})}{M}\times\exp(L_{\rm E}T_{\rm e}/2L_{\rm D}^2)\right.\\ &\left.-\frac{Q\exp(-\alpha_{h\nu}T_{\rm e})}{M} - \alpha_{h\nu}L_{\rm D}\exp(-\alpha_{h\nu}T_{\rm e})\right\}, \end{aligned} \tag{8}$$

where $L_{\rm E}$ is the electron drift length under the electronic field for exponential GaAs photocathodes,[13]

$$\begin{aligned} &L_{\rm E} = \mu\,|E|\,\tau = \frac{q\,|E|}{kT}L_{\rm D}^2,\\ &N = \sqrt{L_{\rm E}^2 + 4L_{\rm D}^2}, \quad S = S_{\rm V} + \mu\,|E|\,,\\ &M = \frac{ND_{\rm n}}{L_{\rm D}}\cosh\left(\frac{NT_{\rm e}}{2L_{\rm D}^2}\right) + \left(2SL_{\rm D} - \frac{D_{\rm n}L_{\rm E}}{L_{\rm D}}\right)\\ &\quad\times\sinh\left(\frac{NT_{\rm e}}{2L_{\rm D}^2}\right),\\ &Q = SN\cosh\left(\frac{NT_{\rm e}}{2L_{\rm D}^2}\right) + (SL_{\rm E} + 2D_{\rm n})\\ &\quad\times\sinh\left(\frac{NT_{\rm e}}{2L_{\rm D}^2}\right). \end{aligned} \tag{9}$$

The coefficients in Eqs. (7) and (8) are each shown as a function of Eq. (9).

3. Experiments and analyses

In order to verify the equations for transmission-mode GaAs photocathodes of exponential doping structure, we designed one transmission-mode material by molecular beam epitaxy (MBE) technology. With the limitation of the epitaxial growth technique, the exponential doping structure was in fact a special kind of gradient doping structure. The thickness of the GaAs active layer was 2 μm, and is divided into eight sections with the p-type beryllium (Be) doping concentrations exponentially varying from 1×10^{18} cm^{-3} to 1×10^{19} cm^{-3} according to Eq. (1) by MBE. The doping structure is shown in Fig. 3. The stopping layer served as an etch-resistant stopping layer and the cap layer was used as an inner oxidation preventing layer. The GaAlAs window layer was designed to have a Be doping concentration of 1×10^{19} cm^{-3} and an Al mole fraction of 0.63. In the whole growing process, the growth rates of GaAs and GaAlAs were both about 1 μm/h and the crystalline quality of the epilayer was also monitored via reflection high-energy electron diffraction.[14,15]

Cap layer	0.1 μm	GaAs	1.0×10^{18} cm^{-3}
Window layer	1 μm	GaAlAs	1.0×10^{19} cm^{-3}
Active layer	0.2 μm	GaAs	1.0×10^{19} cm^{-3}
	0.13 μm	GaAs	8.5×10^{18} cm^{-3}
	0.15 μm	GaAs	7.0×10^{18} cm^{-3}
	0.19 μm	GaAs	5.5×10^{18} cm^{-3}
	0.25 μm	GaAs	4.0×10^{18} cm^{-3}
	0.31 μm	GaAs	2.7×10^{18} cm^{-3}
	0.36 μm	GaAs	1.7×10^{18} cm^{-3}
	0.41 μm	GaAs	1.0×10^{18} cm^{-3}
Stopping layer 1 μm GaAlAs no-doping			
High-quality p-type GaAs(100) substrate			

Fig. 3. Diagram showing the transmission-mode material of the exponential doping structure.

After growth, the cap layer was first removed with a proper etch to expose the GaAlAs window layer for coating the Si_3N_4 antireflection film onto it. After the coating layer was applied to the surface of the window layer, the glass was thermo-compression

bonded to the full wafer structure. Finally, the substrate and stopping layer were selectively etched away to expose the active layer in order to perform activation. During the seal procedure, the transmission-mode GaAs photocathode module was made into a glass/ Si_3N_4/GaAlAs/GaAs structure, as shown in Fig. 4.[16]

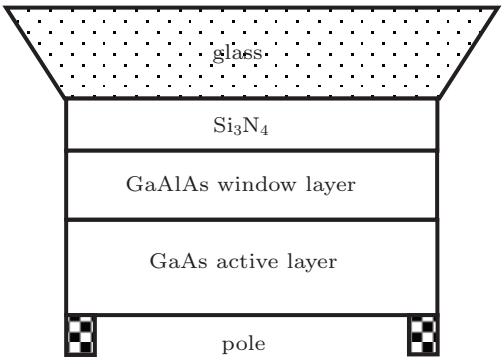


Fig. 4. Diagram showing the GaAs photocathode module of the transmission mode.

Before measuring the SPV curve, the GaAs photocathode material had to be ultrasonically washed in acetone, hydrofluoric acid and absolute ethyl alcohol, in sequence, in order to wipe off the surface oxidation layer and impurities. As shown in Fig. 5, the surface photovoltage measurement system consists of a light source, a lens, a grating monochromator, a photovoltage pond, a lock-in amplifier, a light chopper, a computer and measuring software, etc. When the system began, light from the source passed through the lens and entered into the light chopper, and the light was modulated by the chopper into alternate light. The chopped light passed through the grating monochromator and was converted into monochromatic light, which finally irradiated the samples. The surface photovoltage signal was amplified by a lock-in amplifier and collected by a computer. The scanning rate and sample temperature were also controlled by computer. The whole system can ensure the accuracy and validity of measuring the parameters of the cathode materials. Because the surface photovoltage was measured directly on the GaAs active layer surface before the window layer and the Si_3N_4 cap layer were grown, the influence of these layers, such as the absorption coefficient of the window layer, could not be taken into account. Thus, we measured the surface photovoltage of the GaAs active layer exactly.[17]

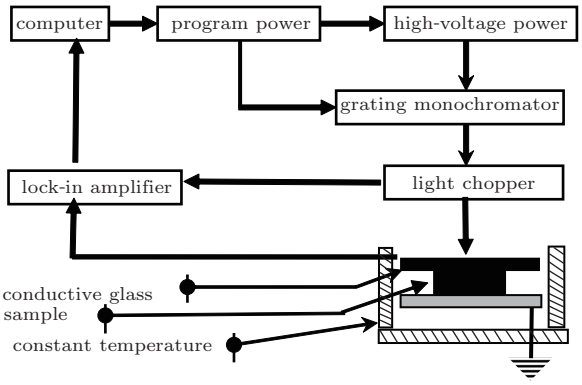


Fig. 5. Diagram showing the surface photovoltage measurement system.

The experimental curve and fitting curves of the surface photovoltage following Eq. (7) are shown in Fig. 6.

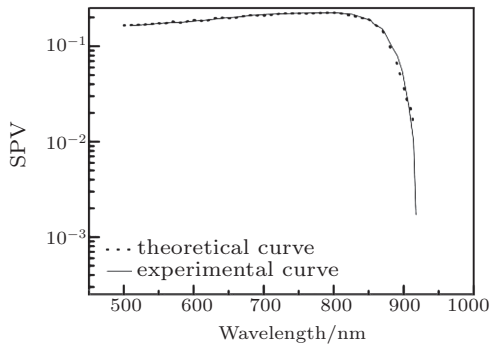


Fig. 6. Theoretical fitting and experimental curves of the surface photovoltage for exponential doping material.

In order to be distinguished from the electron drift length of the uniform doping photocathode, the electron diffusion and drift length $L_{\rm DE}$ is defined as a function of electron drift length $L_{\rm E}$ and electron diffusion length $L_{\rm D}$, and expressed as[18]

$$L_{\rm DE} = \frac{1}{2}\left(\sqrt{L_{\rm E}^2 + 4L_{\rm D}^2} + L_{\rm E}\right). \tag{10}$$

From Eq. (7), we can obtain the fitting parameters of the exponential doping material, such as electron diffusion length and back-interface recombination velocity, as shown in Table 1.

Table 1. The fitting parameters of the exponential doping material through SPV before activation.

$A/\mu m^{-1}$	$D_n/\mu m^2 \cdot s^{-1}$	$T_e/\mu m$	$S_V/\mu m \cdot s^{-1}$	$L_D/\mu m$	$L_{DE}/\mu m$
1.15	1.2×10^{10}	2	1×10^{10}	1.51	3.31

Before Cs–O activation, the photocathode module must go through chemical cleaning and heating

treatment in vacuum in order to remove surface contamination such as carbon and oxides. Thus, the GaAs photocathode material was activated through high–low temperature steps: the temperatures were 600 °C and 410 °C. The heating time was about one hour and the vacuum was above 1×10^{-6} Pa. When the temperature was cooled naturally to below 60 °C, the vacuum returned to above 1×10^{-7} Pa. The Cs–O activation was carried out according to the principle that the Cs source is continuous and the O source is discontinuous. The entire surface potential barrier comprises two stages, which are called stage I and stage II, corresponding to the initial Cs activation and the Cs–O alternate activation as shown in Fig. 2. During the initial stage of Cs activation, the adsorption of Cs on the cathode surface reduces the surface vacuum level to zero electron affinity. With a further increase in Cs coverage, over-shoot behavior occurs as a result of the effects of depolarization and metallic phase transition, which causes the scattering of photoelectrons in metallic Cs islands, thereby hindering the surface electron from escaping. The subsequent codeposition of Cs and O^2 forming the Cs–O dipole layer will further reduce the work function to achieve the final surface NEA state. As a result, the potential barrier II can further drop down to a lower level relative to the bulk conduction-band minimum.[19,20]

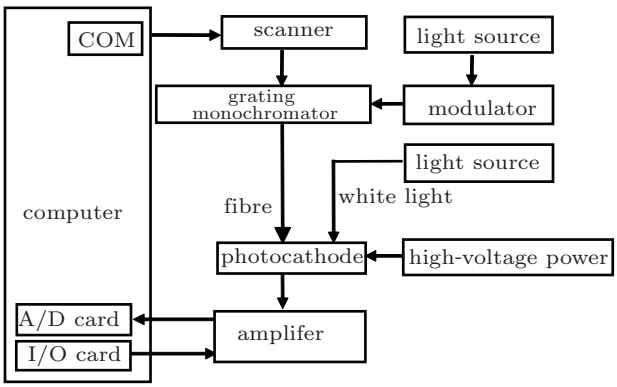


Fig. 7. The spectrum response measurement system after activation.

After activation, the SRC can be measured by the system, as shown in Fig. 7. When the test began, a white light generated by a light source was first modulated to reduce the disturbing signal using a modulator and then grated into a monochromatic light by a grating monochromator. The monochromatic light, which passed through the optical fiber and thus induced the attenuation by a quartz rod, irradiated the surface of the photocathode. The generated photocurrent of the photocathode was collected and amplified by a weak signal detecting circuit and then finally converted into digital signals by an A/D converter. During the whole scanning process from 400 to 1000 nm, the spectral response curve was finally obtained, which is shown in Fig. 8.[21,22]

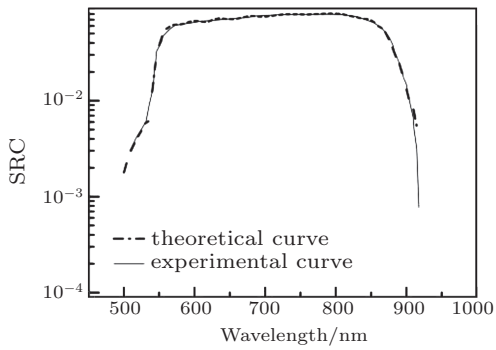


Fig. 8. Theoretical fitting and experimental SRCs for the exponential doping photocathode module.

To fit the spectral response of the exponential doping photocathode module, the influence of the GaAlAs window layer must be removed. Therefore, Eq. (7) must be multiplied by a factor for the absorption coefficient influence of the GaAlAs window layer, which is given as

$$K = \exp(-\beta_{h\nu} T_{\rm w}), \tag{11}$$

where $\beta_{h\nu}$ is the absorption coefficient of the GaAlAs window layer, and $T_{\rm w}$ the thickness of the window layer. The absorption coefficient curve of the GaAlAs window layer is shown in Fig. 9

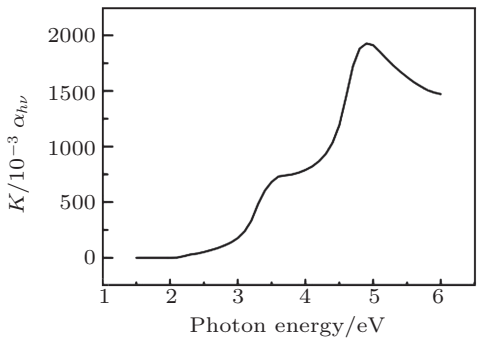


Fig. 9. The absorption coefficient of the $Ga_{1-x}Al_xAs$, $x = 0.63$ window layer.

By using Eq. (8), the fitting parameters for the exponential doping photocathode module are as follows.

Table 2. The fitting parameters of exponential and uniform doping materials by SRC after activation.

$A/\mu m^{-1}$	$D_n/\mu m^2 \cdot s^{-1}$	$T_e/\mu m$	$S_V/\mu m \cdot s^{-1}$	$L_D/\mu m$	$L_{DE}/\mu m$	P
1.15	1.2×10^{10}	2	1×10^{10}	1.51	3.31	0.41

As shown in Table 2, the parameters such as electron diffusion length and back-interface recombination velocity, which are closely related to the body materials of GaAs photocathodes, are directly cited from the SPV fitting calculations shown in Table 1. Only the value of SEP is fitted by the SRC curve. Through the fitting calculations before and after activation, we can find that the curves agree well with the experimental curves, so this comparative research method can help us to better measure the body material and Cs–O activation parameters than the early research method.[23]

Through this comparative research, we can also find that the electron diffusion and drift length L_{DE} is larger than the doubled value of the electron diffusion length L_D. The reason for this is that a constant built-in electric field can form in the active layer due to the exponential doping structure, which will help the photo-excited electrons move toward the surface barriers through both diffusion and electric directional drift in the body electric field. Thus, the electron average transport distance of the exponential doping photocathode within the minority carrier lifetime can be enhanced, which is in contrast to the early uniform doping structure. Finally, the photon emission capability is improved due to the increases in transport efficiency and the chance for low-energy photoelectrons to tunnel through the surface barriers. The SEP value can also be elevated because the photoelectrons reaching the surface band-bending region can gain additional energy from the body electric field in the GaAs bulk, which will help the photo-excited photoelectrons escape the surface barriers more easily than in the case of the uniform doping structure with no body electric field. The influence of doping structure on SEP will be studied more thoroughly in the future.[24,25]

4. Conclusions

By solving the one-dimensional diffusion equation for no equilibrium minority carriers of transmission-mode GaAs photocathode material, we can deduce the equations for the SPV before Cs–O activation and the SRC after Cs–O activation. Through experiments and fitting calculations for the designed exponential doping structure material, body-material parameters such as electronic diffusion length and back-interface recombination can be exactly fitted by the SPV before activation. Furthermore, the SEP value can be well fitted by the comparative research between SPV before activation and SRC after activation. This comparative measurement method can test and characterize the body materials and activation technique well compared with the early research method of only measuring the parameters by SRC, which cannot separate the body materials from activation. The influences of the exponential doping structure on the emitting performance of the cathode are also discussed. This comparative research method will help us to study the varied doping technique and improve the activation technique for transmission-mode GaAs photocathodes in the future.

Acknowledgement

The authors would like to thank Yiping Zeng of the Institute of Semiconductors, Chinese Academy of Sciences, for supplying the transmission-mode GaAs sample, and Shi Feng *et al.* of the Xian Institute of Applied Optics for assistance in the experiments.

References

[1] Zou J J, Chang B K and Yang Z 2007 *Acta Phys. Sin.* **56** 2992 (in Chinese)
[2] Yang Z, Chang B K, Zou J J, Qiao J L, Gao P, Zeng Y P and Li H 2007 *Appl. Opt.* **4** 67035
[3] Kudman I and Seidel T 1962 *J. Appl. Phys.* **33** 771
[4] Zeng Y P, Cao X, Cui L J, Kong M Y, Pan L, Wang B Q and Zhu Z P 2001 *J. Cryst. Growth.* **210** 227
[5] Pollehn H K 1995 *Adv. Electron. El. phys.* **64A** 63
[6] Niu J, Zhang Y J, Chang B K, Yang Z and Xiong Y J 2009 *Appl. Opt.* **48** 5445
[7] Zhang Y J, Chang B K, Yang Z, Niu J and Zou J J 2009 *Chin. Phys.* B **18** 4541
[8] Zhang Y J, Niu J, Zou J J, Chang B K and Xiong Y J 2010 *Appl. Opt.* **49** 3935
[9] Mulhollan G A, Subashiev A V, Clendenin J E, Garwin E L, Kirby R E, Maruyama T and Prepost R 2001 *Phys. Lett.* A **282** 309

[10] Zou J J, Chang B K, Chen H L and Liu L 2007 *J. Appl. Phys.* **101** 033121

[11] Niu J, Zhang Y J Chang B K and Xiong Y J 2011 *Chin. Phys.* B **20** 044209

[12] Olafsson H O Gudmundsson J T Svavarsson H G and Gislason H P 1999 *Physica* B **273** 689

[13] Zhang Y J, Niu J, Zhao J, Zou J J, Chang B K, Shi F and Cheng H C 2010 *J. Appl. Phys.* **108** 093108

[14] Foussekis M, Ferguson J D, Baski A A, Morko H and Reshchikov M A 2009 *Physica* B **23** 4892

[15] Antypas G A, James L W and Uebbing J J 1970 *J. Appl. Phys.* **41** 2888

[16] Liu Y Z, Moll J L and Spicer W E 1970 *Appl. Phys. Lett.* **17** 60

[17] Kronik L and Shapira Y 2001 *Surf. Interface. Anal.* **31** 954

[18] Daniela C, Saurabh P, Beatrice F and Anna C 2011 *Appl. Phys. Lett.* **98** 142111

[19] Drouhin H J, Hermann C and Lampel G 1985 *Phys. Rev.* B **31** 3859

[20] Pastuszka S, Kratzmann D, Schwalm D, Wolf A and Terekhov A S 1997 *Appl. Phys. Lett.* **71** 2967

[21] Liu Z, Sun Y, Peterson S and Pianetta P 2008 *Appl. Phys. Lett.* **92** 241107

[22] Farsakoglu O F, Zengin D M and Koalas H 1993 *Opt. Eng.* **32** 1105

[23] Reshchikov M A, Foussekis M and Baski A A 2010 *J. Appl. Phys.* **107** 113535

[24] Tereshchenko O E, Voronin V S, Scheibler H E, Alperovich V L and Terekhov A S 2002 *Surf. Sci.* **51** 507

[25] Tomkiewicz P, Arabasz S, Adamowicz B, Miczek M, Mizsei J, Zahn D T, Hasegawa H and Szuber J 2009 *Surf. Sci.* **603** 498